Geodynamic significance of the updated Statherian–Calymmian (at *c.* 1.65 and 1.46 Ga) palaeomagnetic results from mafic dykes of the Indian shield

T. Radhakrishna[1,]* and Ram Chandra[2]

[1]National Centre for Earth Science Studies, Thiruvananthapuram 695 031, India
[2]Centre of Excellence in Geology, Institute of Earth Science, Bundelkhand University, Jhansi 284 128, India

A reassessment of the recent palaeomagnetic data on Proterozoic mafic dykes in the Bundelkhand and Bastar cratons permits a robust estimate of 1.466 Ga (Calymmian) pole (λ = 49.4°N; ϕ = 132.9°E; A_{95} = 6.6°; N = 11) for the Indian shield. The pole corresponds to a mean direction of D = 40.5°; I = 56.4° (α_{95} = 5.5°; K = 70). The Indian pole at *c.* 1.65 Ga (Statherian) is suggested to have been situated at λ = 59.6°N and ϕ = 47.9°E (A_{95} = 8.1°; N = 6); it is estimated from a mean direction of D = 336.4°; I = 66.0°N (α_{95} = 5.3°; K = 159). The 1.466-Ga-old dykes are confined to the Eastern Ghats orogenic front in the easternmost part of the Bastar craton. Geochemically, the shoshonitic/high-K calc-alkaline affinity of these dykes is uniquely distinct from the tholeiitic composition found in Meso- or Palaeoproterozoic dykes in other parts of the Indian shield. Testing the existing pre-Rodinia Mesoproterozoic tectonic reconstructions negates the Columbia reconstructions in which the Indian shield is shown in juxtaposition with North China/Laurentia. On the other hand, palaeomagnetic and geological data suggest that the linkages between the Indian shield and Western Australia proposed earlier for the Palaeoproterozoic appear to persist during the Mesoproterozoic as well. The linkages may be further extended into Baltica.

Keywords: Geodynamics, mafic dykes, orogenic belts, palaeomagnetism, tectonic reconstructions.

LATE Palaeoproterozoic and Mesoproterozoic earth history is the subject of current interest following proposals for a Pre-Rodinia supercontinental assembly variably designated as Nuna, Hudsonland or Columbia (e.g. references 1–11 and references therein). Most of these models rely on geological evidences, particularly the distribution of 1.8–2.1 Ga orogenic belts. The reconstructions are highly speculative and sometimes technically incorrect mainly due to paucity of high-quality Late Palaeoproterozoic and Mesoproterozoic palaeomagnetic data. The data are insufficient even to draw an apparent polar wander (APW) path for any single craton[12]. Piper[13], on the other hand, argues for quasi-integral property of palaeomagnetic pole positions across most Precambrian shields for over 2 Ga, challenging the popular models of 'Rodinia' and 'Columbia' supercontinents as well as the general thesis of 'supercontinent cycles'.

The Indian shield comprises Archaean cratons notably Dharwar, Bundelkhand, Bastar and Singbhum. Recent works that can be linked to high-precision U–Pb geochronology have increased the Precambrian palaeomagnetic database from India[14–19]. These results are restricted to the early–middle Palaeoproterozoic Era. The only study that pertains to the Late Palaeoproterozoic to Mesoproterozoic eras has been done by Pisarevsky *et al.*[12] from dykes yielding a U–Pb age of 1466.4 ± 2.6 Ma on the Bastar craton. The authors reported steep upward/downward magnetization directions from these dykes. Additional studies[17–19] also yielded steep palaeomagnetic directions for dykes in the Dharwar, Bundelkhand and Bastar cratons. However, analysis of this larger set of steep directions allows for the identification of four subsets within the steep magnetization. While two subsets (named steep 1 and steep 2) are clearly identified as Early Palaeoproterozoic (Radhakrishna *et al.*[18] and references therein) and one of the subsets (steep 3) could be of Neoproterozoic age, one direction (steep 4) could not be assigned any age and is described to be of unknown age. A few dykes with moderately steep directions spatially closer to steep 3 or steep 4 directions but statistically different from these groups have remained ambiguous. We find that the moderately steep magnetization is statistically in remarkable agreement with the results reported for the 1466.4 ± 2.6 Ma dykes[20], while magnetization of the four dykes reported by Pisarevsky *et al.*[12] overlaps steep 1, steep 2 or steep 4 directions. Here we update the palaeomagnetic record of this early Mesoproterozoic period based on the analysis of combined data. This revised pole position significantly improves the palaeopole record for the Indian shield. We further use the pole data to constrain the tectonic reconstructions during this period.

*For correspondence. (e-mail: tradha1@rediffmail.com)

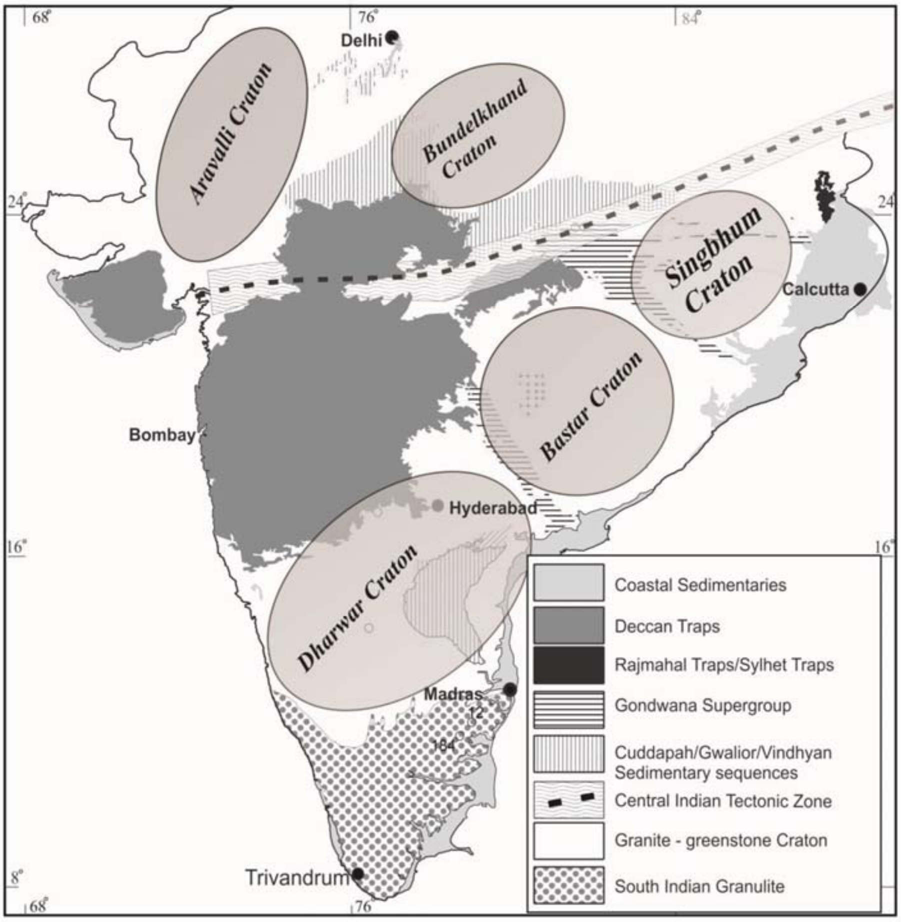

Figure 1. Tectonic sketch of the Indian shield showing the Archaean cratons and major geological features.

Geological background

A detailed account on the geological setting of dykes in the Dharwar, Bundelkhand and Bastar cratons is given elsewhere[12,15–18]. Only salient aspects are summarized here. The Bastar craton together with the Dharwar and Singbhum cratons amalgamated with the Bundelkhand–Aravalli craton along the Central Indian Tectonic Zone (CITZ) prior to 2.45–2.5 Ga (Figure 1). Subsequent movements, if any, along the CITZ are only minor. Although a few authors[21–23] propose continental-scale tectonics in post-2.5 Ga periods[21–23], the arguments are not in agreement with recent palaeomagnetic data[15–17,24]. Basement in these cratons constitutes Archaean gneissic rocks enclosing different greenstone assemblages of variable dimensions (see exhaustive reviews in refs 25, 26). The Proterozoic Eastern Ghat Mobile Belt (EGMB) is a distinct tectonic unit on the southeastern margin of Bastar craton separated from the main cratonic elements of the Indian shield. The EGMB amalgamated with the Indian shield during late Meso- and Neoproterozoic times[27,28]. Nearly flat-lying Palaeoproterozoic sedimentary basins known as Purana basins are distributed along the cratonic margins[29]. Mafic dykes generally do not penetrate into the sedimentary sequences of the basins.

Mafic dykes are widespread in the Bundelkhand, Bastar and Dharwar cratons (Figure 1). High-precision U–Pb geochronology of these dykes is limited. An integration of the available U–Pb baddeleyite/zircon geochronology[16,30] and palaeomagnetic results[14–19] suggests distinct events of Palaeoproterozoic dyke magmatism at about 2.45, 2.37, 2.21, 1.99–1.89 and 1.86 Ga in these cratons. The 2.22 and 1.86 Ga magmatism is also predominant in the Dharwar craton whereas in the Bundelkhand craton the 2.22 Ga dyke magmatism appears to be less predominant and the 1.86 Ga dykes are not present at all. Radhakrishna *et al.*[17] have reported another event of distinct dyke emplacement based on palaeomagnetic results in the Bundelkhand craton for which an age could not be assigned. In addition, a few dykes in the Lakhna area of the eastern Bastar craton (Figure 1) represent an entirely different magnetization dated at 1466.4 ± 2.6 Ma by U–Pb baddeleyite geochronology[12,20]. All the dated dykes are near N–S trending and include three rhyolites and one coarse gabbro. In the same area, NW/N–SE/S trending dolerite dykes also occur, but no age data are available

Table 1. Comparison of major and trace elements at basalt compositional range between the shoshonite-high-K calc-alkaline affinity (1.466 Ga) dykes and subalkaline tholeiites (Palaeoproterozoic) dykes in the EGMB front of the Bastar craton

	Steep-4 (1.65 Ga)		Steep 1 and steep 2 (2.37 and 2.45 Ga)		Overprint (1.466 Ga)	High-K-type (1.466 Ga)	
Elements	Average (9)	SD	Average (4)	SD	BS15	Average (5)	SD
SiO_2	49.15	1.99	47.78	2.42	51.15	52.62	2.65
TiO_2	1.72	1.09	2.39	1.03	1.01	1.55	0.83
Al_2O_3	14.35	0.70	13.43	0.35	12.18	16.14	1.68
Fe_2O_3	**13.18**	**1.27**	**15.75**	**0.49**	**14.83**	**11.11**	**1.33**
MgO	6.33	0.96	5.45	0.76	7.17	1.86	1.58
CaO	**9.75**	**0.94**	**9.08**	**0.90**	**9.31**	**3.43**	**2.09**
Na_2O	2.30	0.32	2.25	0.15	2.16	4.58	3.03
K_2O	**1.12**	**0.71**	**1.24**	**1.02**	**0.75**	**5.46**	**1.28**
P_2O_5	0.29	0.34	0.51	0.55	0.14	0.50	0.55
MnO	0.19	0.02	0.23	0.02	0.18	0.24	0.11
LOI	2.31	0.37	1.62	0.43	nd	2.11	0.36
Total	100.67		99.72		98.88	99.60	
Sc	27	15	31	16	41	13	11
V	**243**	**30**	**294**	**86**	**299**	**47**	**31**
Cr	216	111	120	106	261	105	83
Co	44	4	55	8	52	20	20
Ni	53	23	28	12	152	11	5
Rb	**41**	**23**	**43**	**19**	**26**	**112**	**36**
Sr	**275**	**261**	**352**	**302**	**115**	**1168**	**1057**
Y	**25**	**9**	**34**	**6**	**24**	**52**	**29**
Zr	**92**	**30**	**147**	**29**	**51**	**574**	**454**
Nb	**15**	**14**	**21**	**12**	**6.9**	**131**	**125**
Ba	**139**	**68**	**265**	**102**	**180**	**1767**	**1760**
La	**22.33**	**7.90**	**22.30**	**15.60**	**8.19**	**112.70**	**85.62**
Ce	**49.00**	**17.94**	**51.58**	**35.45**	**20.08**	**234.30**	**171.10**
Pr	**4.98**	**2.32**	**5.67**	**4.27**	**2.28**	**20.88**	**12.68**
Nd	**26.13**	**9.12**	**26.78**	**16.56**	**13.09**	**96.64**	**60.56**
Sm	**5.91**	**0.58**	**6.02**	**2.29**	**3.48**	**19.28**	**13.11**
Eu	**2.11**	**0.93**	**2.22**	**1.42**	**1.15**	**6.00**	**2.76**
Gd	**4.93**	**0.79**	**6.13**	**1.31**	**4.78**	**13.15**	**7.30**
Tb	**1.09**	**0.66**	**0.97**	**0.15**	**0.84**	**1.59**	**0.71**
Dy	**4.39**	**0.92**	**5.76**	**0.56**	**4.79**	**9.48**	**5.06**
Ho	0.83	0.26	1.12	0.14	1.03	1.69	0.93
Etr	2.50	0.96	3.15	0.65	3.35	4.15	1.97
Tm	0.29	-	0.49	0.11	0.57	0.41	0.03
Yb	2.19	0.93	2.91	0.71	3.21	3.27	1.22
Lu	0.74	0.87	0.48	0.11	0.47	0.49	0.15
Hf	**3.50**	**0.56**	**5.13**	**2.59**	**1.31**	**22.62**	**22.80**
Th	**3.66**	**2.61**	**4.05**	**3.75**	**2.38**	**14.64**	**11.30**
U	1.71	2.46	1.13	1.19	0.27	3.34	2.579341

Source: Pisarevsky *et al.*[12] combined with the present authors' data for BS15 and steep 4 pmag dykes in Bundelkhand. Elements for which differences are prominent are shown in bold.

for them. These dolerites may represent the northeastern extension of the Palaeoproterozoic dolerite dyke swarms in the Bastar craton. It is not possible to distinguish unequivocally the distinct groups of dolerite dykes based on their field disposition. All dykes are massive, dark, coarse dolerites and have gabbroic grain size in the central portions of large dykes. The dykes occur predominantly with NW (to NNW)–SE (to SSE) strike directions with a subordinate number having orthogonal trends. The dykes, by their age grouping, do not appear to have any preferential strike trends. One long ENE trending dyke in Bundelkhand has yielded a Neoproterozoic age (1113 ± 7.4 Ma[16].

Geochemistry

The Lakhna dyke magmatism constitutes both mafic and felsic compositions; it is represented mainly by rhyolites and trachytes with subordinate andesitic to basaltic variants[31]. Pisarevsky *et al.*[12] reported major and trace element geochemistry for these dykes. Most of the N–S dykes possess shoshonitic and high-K calc-alkaline affinities consistent with subduction-related characteristics. Their K_2O content is always high (3.7–9.4 wt%). A comparison of the geochemical data from these N–S trending Mesoproterozoic dykes and the NW–SE trending (and a few N–S trending) dykes allows for the following observations: The NW (or N–S) dolerites are quite different in composition from the 1.466 Ga-old N–S dykes. This set of dykes is of subalkalic tholeiitic basalts with typically low K_2O content (<2.8 wt%). Table 1 exemplifies the distinctions between the two groups. The rare earth element (REE) plots of the two groups show contrasting patterns of light to heavy REE fractionation and Eu anomaly (Figure 2). Mantle-normalized patterns (Figure 3) also produce clear distinctions; the 1.446 Ga N–S dykes are highly enriched compared to the NW–SE (or N–S) trending dolerites. In comparison, Palaeoproterozoic dykes in the Indian shield, including those of the Bastar craton, are subalkalic tholeiitic basalts in composition[32–38] (also unpublished data of the present authors). Thus, it is evident that the N–S trending 1.466 Ga dykes with shoshonitic/high-K calk-alkaline affinity have their spatial distribution restricted to the Bastar basement near to the EGMB front.

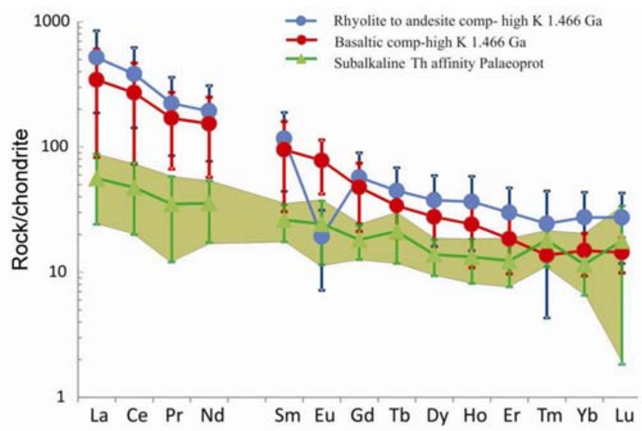

Figure 2. Chondrite-normalized, rare-earth element patterns of the N–S alkaline dykes and the NW–SE trending dolerites of subalkaline tholeiitic basalt composition dykes in the Bastar craton. (Source: Pisarevsky *et al.*[12] and the present authors' unpublished data; normalization values from Sun and McDonough[64].)

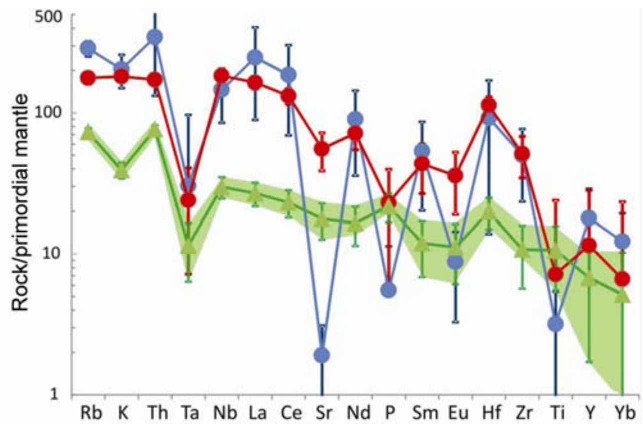

Figure 3. Primordial mantle-normalized, multi-element diagram of the N–S alkaline dykes and the NW–SE trending dolerites of subalkaline tholeiitic basalt composition dykes in the Bastar craton. (Source: Pisarevsky *et al.*[12] and authors unpublished data; Normalization values from Sun and McDonough[64].)

Palaeomagnetism

Palaeomagnetic techniques involve alternating field and thermal demagnetization experiments and the principal component analysis of the consecutive data points defining the linear segments of the demagnetization steps to delineate characteristic remnant magnetizations (ChRM). Full details regarding methods and data analysis are given elsewhere[12,17]. Most of the palaeopoles derived from dykes in the Indian cratonic elements belong to multiple dyke emplacements of Palaeoproterozoic age. Pisarevsky *et al.*[12] grouped a set of steep directions from 10 dykes to define a Mesoproterozoic (1.466 Ga; U–Pb zircon date) direction in the Bastar craton. However, the palaeopoles from these dykes display large scatter both in latitude (1–68°) and longitude (40–130°) and have steep upward/downward directions. Radhakrishna *et al.*[17] also obtained comparable directions from both the Bundelkhand and Bastar cratons. We subdivide these results into four subsets based on the analysis of a large dataset of similar directions from the Dharwar craton[18]. The steep 1 (poles in the equatorial region with long. <80°) and steep 2 (poles in the equatorial region with long. >80°) directions are described to correspond to *c.* 2.37 and 2.45 Ga respectively. In the Bundelkhand craton, five dykes have yielded another distinct but coherent group of directions from these two groups, and are classified into a discrete group of steep 4 magnetization. The 1.446 Ga directions cannot be clearly demarcated into a distinct group from the rest of the steep directional groups in the stereographic plot (Figure 4). Spatially these distinctions are better illustrated in terms of pole distributions and therefore the pole data are plotted in Figure 5. The palaeopoles from some of the dykes reported by Pisarevsky *et al.*[12] overlap with those of other groups of directions (steep 1, steep 2 or steep 4). Four dykes are removed from the rest of the population by more than 40°. Palaeopole estimates from individual dykes define virtual geomagnetic poles and such significant variation can be attributed to the effects of palaeosecular variation. However, the palaeopoles from these dykes are statistically well classified into other palaeopole groups from the craton; geochemically too these dykes are tholeiites similar to dykes of steep 1, 2 and steep 4 groups in contrast to shoshonite compositions of the Mesoproterozoic dykes (Table 1). Dyke D8 pole of their study[12] overlaps poles of steep 1 direction, whereas dyke D2 and D7 poles embrace the steep 2 group of poles (Table 2 and Figure 5); these poles are considered here to belong to steep 1 and steep 2 groups. One dyke (D4) falls into steep 4 group as described below.

One dyke (BS15; Table 2 and Figure 5) in the present study, in the northeast Bastar craton in close vicinity to the Lakhna area of study by Pisarevsky *et al.*[12], has yielded a palaeopole closely comparable to the 1.466 Ga pole (Figure 5). Dyke BS15 and also dyke D9 have compositionally subalkalic affinity as in the Palaeoproterozoic dykes without the shoshonitic affinity displayed by the 1.466 Ga dykes (Table 1). Therefore, it is likely that the magnetization of these two dykes represents an overprint, or alternatively, isolated tholeiitic magmatism of 1.466 Ga in eastern Bastar. In addition, compilation of palaeopole data from Dharwar craton shows that palaeopoles from four dykes notably close to this group of poles (Figures 4 and 5). The data are accordingly updated and listed in Table 2. Altogether 11 dykes from the Indian shield comprise this group defined by a mean direction of $D = 40.5°$; $I = 56.4°$ ($\alpha_{95} = 5.5°$; $K = 70$) yielding a palaeopole of $\lambda = 49.4°$N; $\phi = 132.9°$E ($A_{95} = 6.6°$; $N = 11$). The pole data include both polarities (Table 2) that are mutually antipodal and pass the reversal test[39] of 'Rb' class with an angular difference (γ_0) of 6.3° ($\gamma_{crit} = 13.9°$). Dyke D5 dated at 1.46 Ga (U–Pb zircon date of 1466.4 ± 2.6 Ma)[12] belongs to this group.

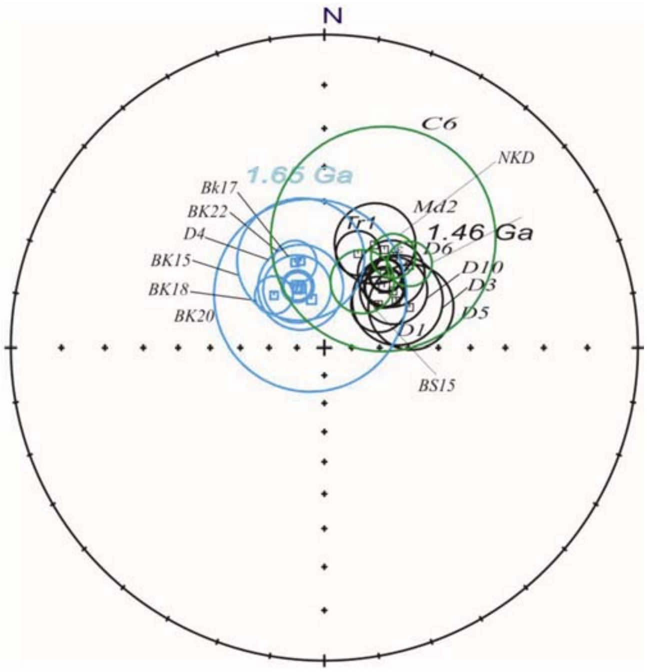

Figure 4. Equal-area projection of directions of magnetization from *c*. 1.65 and 1.46 Ga dykes of the Bastar and Bundelkhand cratons showing mean characteristic remanent magnetisation with α_{95} confidence circles. Antipodal directions for all negative inclination directions are plotted to depict the differences between the 1.65 and 1.46 Ga directions.

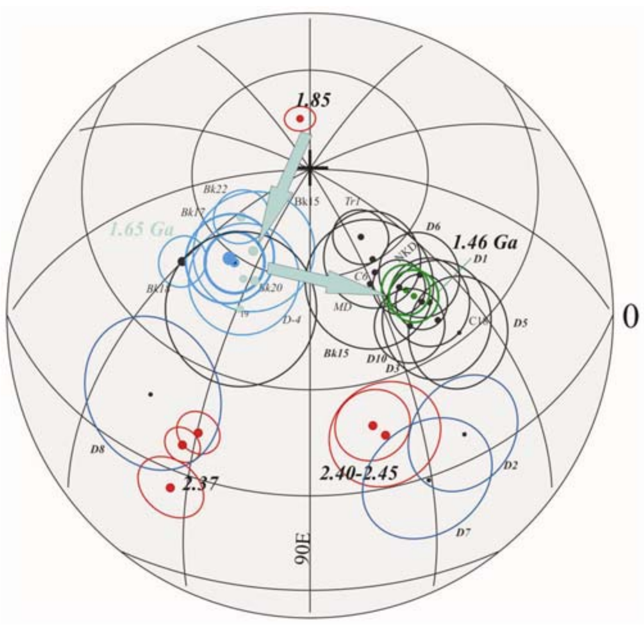

Figure 5. Distribution of palaeomagnetic poles with mean poles for *c*. 1.65 and 1.466 Ga for the Indian shield. The 1.85, 2.37 and 2.45 Ga palaeomagnetic poles[18] are also plotted for comparison. Note that the poles of dyke D8, and dykes D2 and D7 embrace the mean poles of 2.37 and 2.45 Ga respectively.

Dyke D4 in the northeastern Bastar craton is geochemically tholeiite in composition and is quite different from the dykes of shoshonitic affinity linked to 1.466 Ga. Its pole data coincide well with steep 4 poles and is statistically distinct from the 1.466 Ga pole (Figure 5). Dyke D4 and steep 4 dykes share similar major and trace element chemistry (Table 1). Therefore, dyke D4 is grouped with the steep 4 dykes. This group of directions, although reported, did not form a part of the discussion in our earlier work[17] on Palaeoproterozoic intrusions. Out of six dykes, five show good within site grouping ($\alpha_{95} = 6.6$–$16.2°$; $K = 18$–103). Dyke BK20 has higher uncertainty ($\alpha_{95} = 33°$; $K = 9$), but is classified into steep 4 group of directions as the site mean value is within the α_{95} circle over the mean value of this group (Figure 5). The mean palaeopole calculated excluding this dyke ($\lambda = 59.7°$N; $\phi = 48.1°$E) is indistinguishable from the mean pole calculated from all six dykes. Thus, a mean value of the steep 4 direction for the Indian shield is computed using results from the six dykes as $D = 336.4°$; $I = 66.0°$ ($\alpha_{95} = 5.3°$; K = 159). The corresponding palaeopole is situated at $\lambda = 59.6°$N; $\phi = 47.9°$E ($A_{95} = 8.1°$; $N = 6$). Among the six dykes in this subgroup, one is antipodal. These directions pass reversal test of 'Rci' class with $\lambda_0 = 13.2°$ ($\gamma_{crit} = 24.5°$). The high degree of coherence between the pole estimates of the independent dykes distributed over a large area and the positive reversal test suggest that this palaeopole corresponds to the geomagnetic field of a specific geological age. The pronounced within-site spread in terms of precision parameters at individual site level compared to between-site precision parameters and even a reverse magnetization in one dyke, nevertheless indicates remanence acquisition over a protracted time sufficient to average the geomagnetic secular variation. It is clearly evident that the steep 4 poles and the 1.46 Ga poles constitute two independent sets of pole data and the α_{95} confidence circles of the two pole sets barely overlap. Even the circles with relatively large error do not incorporate α_{95} circles covering the mean of the other set of poles. The poles are also remote from those of the Deccan/Rajmahal Traps that frequently register significant Phanerozoic overprinting of magnetizations in the Indian shield[40,41]; they are also removed from known

Table 2. The 1.65 and 1.46 Ga palaeomagnetic data summary from dykes in the Indian shield

Site	Latitude	Longitude	N	D	I	α_{95}	k	λ	ϕ	dp	dm
BS15	20.4	81.1	5	210.0	–63.0	11.0	49	55.4	120.1	13.6	17.3
D1[a]	20.8	82.7	10	50.6	58.4	11.4	19	43.2	138.0	12.5	16.9
D3[a]	20.8	82.7	10	57.1	59.5	15.3	11	38.1	137.1	17.3	23.0
D5[a]	20.8	82.7	7	64.9	56.6	14.2	19	32.0	141.0	14.9	20.6
D6[a]	20.8	82.7	5	42.2	55.1	11.1	48	50.3	141.5	11.2	15.8
D10[a]	20.8	82.7	14	51.7	65.2	9.7	18	40.8	127.5	12.7	15.7
Tr1[a]	20.8	82.7	11	19.7	54.7	7.4	39	67.5	128.7	7.4	10.5
C6[b]	12.4	75.3	7	208.4	–50.9	34.9	14	57.6	124.4	31.8	47.1
C18[b]	12.3	75.2	11	225.5	–48.5	7.2	48	44.5	135.7	6.2	9.5
NK dykes[c]	12.0	75.8	13	217.0	–50.0	7.2	103	51.0	131.1	6.4	9.6
Mysore dyke 2[c]	14.2	76.4	3	26.0	50.0	13.0	36	60.9	127.2	11.6	17.4
Mean of seven dykes (Pishrevsky *et al.*[12])				45.0	59.8	6.8		46.9	134.3		
Mean of 11 dykes in the Indian shield				40.5	56.4	5.5	70	49.4	132.9	A95 = 6.6	
BK-15	24.1	78.5	6	165.0	–66.0	16.2	13	63.0	56.2	21.7	26.5
BK-17	25.6	78.6	6	335.0	67.0	11.9	33	59.1	46.4	16.3	19.7
BK-18	25.6	78.6	6	316.0	64.0	6.6	103	49.7	30.1	8.4	10.5
BK-22	25.5	78.6	7	341.0	58.0	7.3	86	69.3	32.7	7.9	10.8
BK-20	25.4	78.1	4	345.0	72.0	33.3	9	56.6	63.2	51.8	58.7
D4[a]	20.7	82.7	6	338.5	67.1	14.9	21	56.3	57.5	20.5	24.7
				336.4	66.0	5.3	159	59.6	47.9	A95 = 8	
*D2[a]	20.8	82.7	4	96.0	61.6	14.1	43	9.8	130.5	16.8	21.8
*D7[a]	20.8	82.7	6	293.6	–67.0	12.1	32	1.6	119.1	16.6	20.0
*D8[a]	20.8	82.7	6	93.8	–67.6	13.9	24	18.3	40.8	19.4	23.2

N, Number of samples yielding stable directions constituting the group; D and I declination and inclination (degrees) respectively of the characteristic remnant magnetic directions; k = precision parameter; α_{95}, Radius of the 95% confidence; λ and ϕ Latitude and longitude of the virtual palaeomagnetic poles calculated. [a]Data from Pisarevsky *et al.*[12]; BK and BS denote authors data from Bundelkhand and Bastar cratons reproduced from[17,18]; [b]Data from Radhakrishna and Joseph[65]; [c,d]Data from refs 66 and 67 respectively. *Directions excluded in this study as they overlap the older steep 1 or steep 2 directions. Details in text and Figure 5.

Palaeo- or Neoproterozoic magnetizations recorded from India. The palaeopoles of steep 4 group of magnetizations are considered to constitute another distinct group of *c*. 1.65 Ga magnetization, as discussed in the following section.

Discussion

The presence of pairs of precisely coeval palaeopoles from the same two cratonic blocks can provide palaeomagnetic evidence to suggest that these two cratons drifted together as part of a larger continental shield area[42,43]. Applying this test to the Indian shield, recently reported Palaeoproterozoic poles[14,17,18,44] (and references therein) suggest that the Dharwar, Bastar and Bundelkhand cratons drifted together as a larger continental mass at least since 2.4 Ga. Stein *et al.*[45] have also provided Re–Os isotopic evidence supporting the view that these cratons within the Indian shield were unified by 2.5 Ga. Therefore, the 1.466 Ga palaeopole from these three cratons can be combined to calculate a greater mean palaeomagnetic pole of this age for the Indian shield. Accordingly, the palaeomagnetic pole estimated using data from the three cratons (λ = 49.4°S; ϕ = 132.9°E; A_{95} = 6.6°; N = 11; Table 2) is applicable to the Indian shield as a whole.

Precise U–Pb baddeleyite/zircon age data are not available at present for the mean palaeopole derived for the steep 4 group. However, a *c*. 1.65 Ga age is assigned based on the following: The pole is situated spatially at an intermediate position between the poles of 1.466 and 1.86 Ga for the Indian shield (Figure 5). Assuming a similar polar wander rates during the 1.86–1.46 Ga interval, a *c*. 1.65 Ga age is tentatively estimated for the steep 4 group of magnetizations. Alternatively, a *c*. 2.2 Ga age could be assigned to this pole because it falls between 1.86 and 2.37 Ga poles. However, a palaeopole derived from 2.22 Ga dykes is situated too far away (72°) to suggest a temporal linkage between the steep 4 and 2.22 Ga magnetizations. Further, Rb–Sr isotope study yielded a poorly defined regression line corresponding to 1656 ± 22 Ma on one of the Bundelkhand dykes[24]. Recently, an internal isochron age of 1641 ± 120 Ma was obtained[46] between three mineral fractions and whole rock of a dolerite in the central Indian craton. *In situ* $^{40}Ar/^{39}Ar$ analyses of the dykes in the Bundelkhand craton exhibit a cluster at about 1.65 Ga also[47], while some of the ages are concentrated near a possible ~1.99 Ga emplacement age. The palaeopole location of these dykes is remotely displaced from all other known Proterozoic/Phanerozoic pole data, as described earlier in the text. Interestingly, the steep 4 palaeopoles have been recorded relatively in more number of dykes in the Bundelkhand craton, very scarce in the Bastar craton and are not found in dykes from the Dharwar craton. At the same time, majority of K–Ar ages from the eastern Dharwar craton falls within a narrow

Table 3. Palaeomagnetic poles from North China, Laurentia, Western Australia, Baltica and Siberia used to generate Table 4 and Figure 4

Rock unit	Age (MY)	λ	ϕ	A_{95}/Dp, D_m	Reference
North China					
Xiong'er Group	1780	50.2	263.0	4.5	58
Taihang NNW Dykes	1769 ± 2.5	36.0	247.0	2.8	68
A2 dykes	1769	51.3	281.0	3, 7	57
A1 dykes	1769	38.7	244.6	1, 3	57
Mean of 1770–1780 Ma	**1775 ± 5**	**45.0**	**257.3**	**16**	
Yangzhuang Fm	1560–1440	17.3	214.5	8, 4.1	69
Gaoyuzhuang Fm	1434–1550	5.0	32.0	2.6, 5.1	70
Tieling Fm	**1437 ± 21**	**11.6**	**187.1**	**8.1, 4.9**	**71**
Laurentia					
Molson dykes	**1880**	**27.0**	**219.0**	**4**	**72**
Dubawnt Group	1785 ± 4	7.0	277.0	8	73
Cleaverdikes	1740+5/-4	19.0	277.0	6	74
Sparrow Dykes	1700	12.0	291.0	6.6, 9.4	75
Western Channel Diabase	**1590**	**9.0**	**245.0**	**7**	**58, 74**
Beartooth Mountains dykes 7, 8	1500	–2.5	264.4	11,15	76
Laramie Range Anorthosite	1500	14.0	206.0	3, 6	76
Michikamau Intrusion Combined	**1479 ± 10**	**–1.5**	**217.5**	**5**	**77**
St. Francois Mtns	**1476 ± 16**	**13.2**	**219.0**	**8, 4.7**	**78**
Michikamau Intrusion	**1460 ± 5**	**–0.6**	**215.3**	**5**	**79**
Snowslip Fm	**1450 ± 14**	**–24.9**	**210.2**	**3.5**	**80**
Harp Lake Complex	**1450 ± –5**	**1.6**	**206.3**	**4**	**79**
Purcel llava	**1443 ± 7**	**–23.6**	**215.6**	**4.8**	**80**
Laramie complex and Sherman granite	**1432 ± 15**	**–7.0**	**215.0**	**4**	**81**
Mean of 1430–1480 Ma (7)	**1455 ± 18**	**–6.1**	**214.2**	**10.9**	
Mistastin complex	1420	–1.0	201.0	8	79
McNamara Fm	1401 ± 6	13.5	208.3	6.7	80
Zig-Zag Daland intrusions	1382 ± 2	11.0	240.0	3	82
West Australia					
Plum Tree Volcanics	**1825**	**29.0**	**195.0**	**14**	**83**
Frere Fm	1800	45.2	220.0	1.3/2.4	84
Hamersley Province overprint	1800	35.3	211.9	3.0,3.0	85
Hart Dolerite; Kimberley Block	1762 ± –25	29.0	46.0	24	86
Elgee Fm, Kimberley	1750	–4.4	210.0	3.3, 6.5	87
Tooganinie Formation, N Australia	**1650 ± 3**	**61.0**	**187.0**	**6**	**88**
Emmerugga Dolomite, N Australia	1645	79.0	203.0	6	89
Lawn Hill Formation	1611 ± 4	84.4	80.5	2.6	88
Fraser Dyke	1212 ± 10	55.8	325.7	4.7, 5.2	90
Mount Barren area, Western Au	1205 ± 10	43.6	347.4	11.9, 13.9	90
Baltica					
Svecofennian Mean	**1881**	**41.0**	**233.0**	**5**	**8**
Subjotnian quartz porphyry dYKE	**1630**	**29.0**	**177.0**	**6**	**8**
Lake Ladoga	**1452 ± 12**	**15.0**	**177.0**	**5.5**	**91**
Siberia					
Lower Akitkan	**1878 ± 4**	**31.0**	**99.0**	**4**	**92**
Upper Akitkan	**1863 ± 9**	**23.0**	**97.0**	**2**	**92**
Olenëk mafic intrusions	**1473 ± 24**	**33.6**	**253.1**	**10.4**	**10**

Poles in bold are used for generating Table 4.

range of 1650 ± 25 Ma[48,49] even though these dykes have yielded older U–Pb baddeleyite/zircon ages. It is likely that the K–Ar clock was reset in the eastern Dharwar craton by a 1.65 Ga thermal event, although it does not appear to be expressed in magnetic overprinting, unlike the example of the Bundelkhand craton where magnetic overprinting appears to have been registered. Thus, we argue that the steep 4 palaeopoles represent overprint magnetizations developed at ~1.65 Ga.

The 1.466 and 1.65 Ga palaeopoles of the Indian shield are used as a first-order approximation to test varying pre-Rodinia supercontinent models. The underlying premise of all the models incorporating the supercontinent cycle concept is that the supercontinent assembly resulted

Table 4. Great-circle distances between pairs of palaeomagnetic poles of near isochronous interval for the Indian shield, North China, Laurentia, Baltica, Siberia and Western Australia

	India	North China	Laurentia	Siberia	Baltica	Western Australia
1.86–1.65	52 ± 13		22 ± 14 31 ± 14 (1.88–1.59)	–	**46 ± 11**	**41 ± 20** **33 ± 20 (1.83–1.65)**
1.86–1.46	53 ± 12	**86 ± 24** **68 ± 24 (1.78-1.47)**	**31 ± 14** **33 ± 14 (1.88–1.46)**	**23 ± 14**	**55 ± 11**	–
1.65–1.46	46 ± 15		50 ± 17 34 ± 17 (1.59–1.46)	–	**53 ± 12**	–

In case of North China, Laurentia and Western Australia, values have been corrected to match the age bracket of Indian pole pairs. Bold indicates that age differences are closely comparable (±20%). The actual age bracket values are indicated within parenthesis.

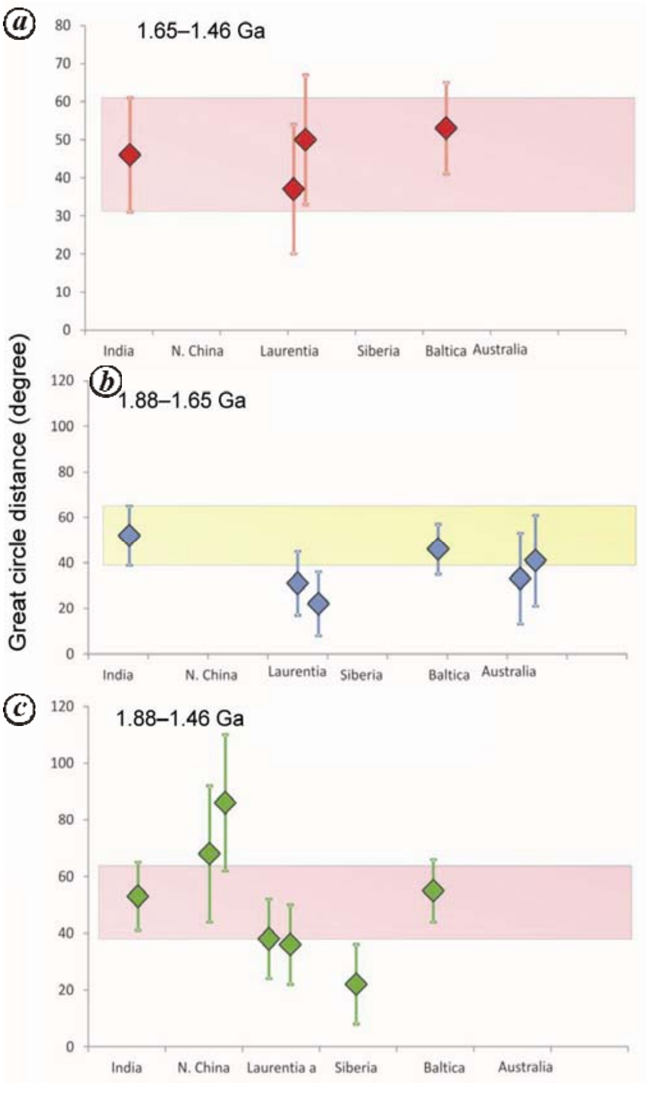

Figure 6. Great-circle distances between pairs of palaeomagnetic poles of near coeval/isochronous interval for the Indian shield in comparison to the same from North China, Laurentia, Siberia, Baltica and Western Australia. The pole distances plotted are listed in Table 3. The angular distances of the Indian shield for paired ages are taken as reference for comparison. Small variations in ages compared to the paired ages in India are calculated assuming the same rate of apparent polar wander for the age bracket. Adjacent to the right of the actual values are the corrected angular distances to match the age bracket of Indian pole pairs. The transparent band represents the great circle distance between the respective pairs of Indian poles with the bounds of error limits.

following the 2.1–1.8 Ga orogenic activity across the globe and persisted up to the end of Mesoproterozoic[11,50–54]. The Indian shield is variously portrayed in the Columbia configurations. Hou *et al.*[55] place the Indian shield adjacent to western margin of Laurentia considering a ~1.85 Ga radiating mafic dyke swarm across these crustal units. In another contrasting configuration[11,56], the Indian shield is positioned adjacent to North China and far away from Laurentia. A North China–India connection was also suggested by palaeomagnetism of 1780–1760 Ma dykes[57] and well-dated Xiong'er Group in North China[58]. In an attempt to evaluate these configurations, here we use the two Mesoproterozoic poles along with 1.86 Ga pole reported earlier[17,18]. We used a comparison of great-circle distances between palaeomagnetic poles (Table 3) of near isochronous interval from these continental blocks (Table 4 and Figure 6) in combination with palaeolatitude distribution during this age bracket (Figure 7) to test the tectonic linkages of the Indian shield. The angular distances between *c*. 1.86 and 1.46 Ga intervals for the Indian shield and North China are not in agreement. These two crustal units are marked by significant geological differences[17,18]. Only one pair of poles is available from Siberia (1.88 and 1.46 Ga) for comparison within the period of this study, and the angular distance between the poles is quite distinct from that of India (Figure 6). In case of Laurentia, the poles of a 1.88–1.47 Ga pair are of greater certainty and the mean angular distance between the poles of this pair is outside the range defined by the comparable pair of poles from India. Since certainty of poles around 1.65 Ga for Laurentia is not clear, the two poles at 1.59 and 1.65 Ga (Table 3) are considered. In both cases, except one data point, all other angular distances of paired poles are on the verge of error limits or away from the angular distance band marking the error limits for India (Figure 6). In the plot of palaeolatitude distribution (Figure 7), the North China and Laurentia palaeolatitudes are distributed in the near equatorial position during *c*. 1.86–1.40 Ga, indicating almost an east–west drift. In sharp contrast, the Indian shield displays a north–south drift with its near equatorial palaeolatitude at *c*. 1.85 Ga spatially moving towards moderately steep latitudes by the early Mesoproterozoic.

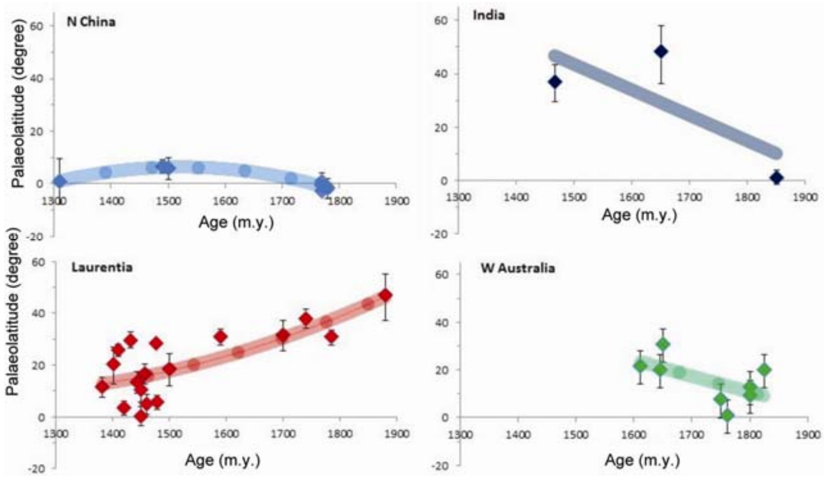

Figure 7. Palaeolatitude estimates between 1.88 and 1.44 Ga along with error bars of α_{95} confidence limits from the Indian shield (top right) compared with the palaeolatitude data from Western Australia (down right), Laurentia (down left) and North China (top left). It is seen that the motion is equator-parallel (or towards the equator) for both Laurentia and North China, in sharp contrast to that of the Western Australia and the Indian shield. Both Western Australia and India move from the equator towards higher latitudes between 1.85 and 1.44 Ga. The pole data plotted are listed in Table 3.

These observations suggest that the drift of the Indian shield is independent from that of North China or Laurentia. Pisarevsky *et al.*[12], while considering different scenarios of the Laurentia/Siberia–India connection, found several lines of geological discordances that negate feasibility of this reconstruction.

A distinct cratonic antiquity demonstrated earlier for the Indian shield from North China and Laurentia during the early to mid Palaeoproterozoic[15–18] appears to be valid during the Mesoproterozoic also, at least until 1.46 Ga. Although pairs of palaeomagnetic poles of near isochronous interval are not presently available for comparisons, the Western Australian group shows a north–south drift like India. Similar palaeolatitude positions for Western Australia (Yilgarn craton) and the Indian shield persisted during the Palaeoproterozoic[14,17,18]. The style of palaeolatitude movement for both India and Australia appears to be similar across the Palaeo- and Meso–Proterozoic boundary (Figure 7). Thus, the Mesoproterozoic reconstructions with the Indian shield attached to Western Australia are favoured over the models proposing close neighbourhood of India and North China/Laurentia. Pisarevsky *et al.*[12] suggested India in juxtaposition with SW Baltica based on agreement of poles at 1.46 and 1.12 Ga and similarity of a few geological features. The angular distances between the three pairs of poles plotted from Baltica and India are remarkably in agreement (Figure 6) suggesting their movement as a single entity. Extensional processes with accompanied basin formation in the Late Palaeoproterozoic both in Australia and India, the presence of significant juvenile felsic volcanic source of 1650 Ma as evident from €Nd values of the Proterozoic detritus in Australian sedimentary successions[59], the *c.* 1630 Ma U–Pb ages of felsic tuffs of volcanic origin in the Proterozoic Vindhyan Basin[60,61], the juvenile magmatism in Baltica at *ca.* 1655 Ma (refs 62, 63) are in agreement with the proposed tectonic linkages. More studies on palaeomagnetism, sedimentary source and timing of juvenile magmatism may further develop the reconstructions suggested here. Nonetheless, the above interpretations disputing India–Laurentia/North China linkages along with other palaeomagnetic inconsistencies in positioning several other cratons (South Africa, Australia or Siberia) differently than in the putative Columbia model[15,16], suggest that the Mesoproterozoic reconstructions warrant significant improvements.

We also evaluated the present results with respect to the Palaeopangaea reconstruction models proposed by Piper[13]. Both poles are rotated according to the Palaeopangaea rotation parameters[13] and none of these poles correlates with the proposed reconstructions (figure not shown). One possible reason for this could be the absence of well-dated Mesoproterozoic poles to constrain the reconstruction models. At the same time, it is interesting that the pole from Calymmian (1.466 Ga) dykes is in broad agreement with *c.* 1 Ga poles when rotated into Palaeopangaea B reconstruction. In this context, it is worth noting that the dykes yielding this pole are close to the tectonic front of the EGMB and it can be argued that they have unlikely escaped Grenville-age remagnetization. If this is the case, the magnetization age of these dykes is different from the U–Pb emplacement age. Field tests are absent at present to confirm the magnetization as primarily linked to their U–Pb emplacement age. However, magnetization in these dykes statistically differs from the recently reported Indian poles at ~1.0 Ga; the dykes towards the EGMB in the Bastar craton still preserve the Palaeoproterozoic directions. Thus, we prefer to argue in favour of linking magnetization to 1.466 Ga U–Pb emplacement age rather than considering it as the

Grenville-age overprint. Mesoproterozoic ages (1381–1430 Ma), remaining intact at about 50 km distance all along the western marginal zone of the EGMB (Figure 2)[28], clearly indicate little possibility for the Grenville age magnetic overprinting in the Lakhna dykes, which are far beyond 50 km to the west of the EGMB.

Conclusions

Here, we have presented an update of the Statherian–Calymmian palaeomagnetic data for the Indian shield. The study reports more robust 1.466 Ga mean palaeomagnetic pole and another pole that corresponds to a possible age of ~1.65 Ga. The pole data have been used to test the pre-Rodinia Mesoproterozoic continental reconstructions based on great-circle distances between palaeomagnetic poles of near-isochronous intervals and palaeolatitude distributions. The analysis suggests that the Indian shield was not attached to the North China/ Laurentia crustal units as proposed in some of the Mesoproterozoic reconstructions. In turn, the Indian shield appears to be in juxtaposition with Australia, as has been demonstrated in the early–mid-Palaeoproterozoic reconstructions. Furthermore, the continental linkage appears to extend into Baltica. The present approach identifies similar angular distances between three pairs of poles coming from India and Baltica, supporting an India–Baltica connection as suggested recently by Pisarevsky *et al.*[12]. More data from future studies may validate the linkage. A proposal suggesting remagnetization of Calymmian (1.466 Ga) dykes at Grenville age, in view of their proximity to the EGMB tectonic front, appears to be in conformity with Palaeopangaea B reconstruction[13], however, such an argument remains equivocal at this stage. Further analysis of recently reported geochemical data suggests that the 1.466 Ga felsic/mafic dyke magmatism has affinity to a subduction-related shoshonite–calc-alkaline and high-K calc-alkaline magmatism, and it is spatially confined to the Bastar craton near the EGMB. This is in sharp contrast to the subalkaline tholeiite composition of the dykes of Palaeoproterozoic age that occur pervasively across the Archaean cratons in the Indian shield.

1. Condie, K. C., Episodic continental growth models: afterthoughts and extensions. *Tectonophysics*, 2000, **322**, 153–162.
2. Hoffman, P. F., Tectonic genealogy of North America. In *Earth Structure: An Introduction to Structural Geology and Tectonics* (eds van der Pliujm, B. A. and Marshak, S.), W. W. Norton & Company, New York, 1996, pp. 607–614.
3. Rogers, J. W. J. and Santosh, M., Configuration of Columbia, a Mesoproterozoic supercontinent. *Gondwana Res.*, 2002, **5**, 5–22.
4. Rogers, J. J. W. and Santosh, M., Tectonics and surface effects of the supercontinent Columbia. *Gondwana Res.*, 2009, **15**, 373–380.
5. Meert, J. G., Paleomagnetic evidence for a Paleo-Mesoproterozoic supercontinent Columbia. *Gondwana Res*., 2002, **5**, 207–215.
6. Meert, J. G., What's in a name? The Columbia (Paleopangaea/Nuna) supercontinent. *Gondwana Res.*, 2012, **21**, 987–993.
7. Evans, D. A. D. and Mitchell, R. N., Assembly and breakup of the core of Paleoproterozoic–Mesoproterozoic supercontinent Nuna. *Geology*, 2011, **39**, 443–446.
8. Pesonen, L. J. *et al.*, Palaeomagnetic configuration of continents during the Proterozoic. *Tectonophysics*, 2003, **375**, 289–324.
9. Pisarevsky, S. A. and Bylund, G., Paleomagnetism of 1780–1770 Ma mafic and composite intrusions of Småland (Sweden): implications for the Mesoproterozoic supercontinent. *Am. J. Sci.*, 2010, **310**, 1168–1186.
10. Wingate, M. T. D., Pisarevsky, S. A., Gladkochub, D. P., Donskaya, T. V., Konstantinov, K. M., Mazukabzov, A. M. and Stanevich, A. M., Geochronology and paleomagnetism of mafic igneous rocks in the Olenek Uplift, northern Siberia: implications for Mesoproterozoic supercontinents and paleogeography. *Precambrian Res*., 2009, **170**, 256–266.
11. Zhao, G., Sun, M., Wilde, S. A. and Li, S., A Paleo-Mesoproterozoic supercontinent: assembly, growth and breakup. *Earth-Sci. Rev*., 2004, **67**, 91–123.
12. Pisarevsky, S. A. *et al*., Palaeomagnetic, geochronological and geochemical study of Mesoproterozoic Lakhna dykes in the Bastar Craton, India: implications for the mesoproterozoic supercontinent. *Lithos*, 2012, **174**, 125–143.
13. Piper, J. D. A, Continental velocity through Precambrian times: the link to magmatism, crustal accretion and episodes of global cooling. *Geosci. Front.*, 2013, **4**, 7–36.
14. Halls, H. C., Kumar, A., Srinivasan, R. and Hamilton, M. A., Palaeoimagnetism and U–Pb geochronology of easterly trending dykes in Dharwar Craton, India: feldspar clouding, radiating dyke swarms and the position of India at 2.37 Ga. *Precambrian Res.*, 2007, **155**, 47–68.
15. Meert, J. G., Pandit, M. K., Pradhan, V. R. and Kamenov, G., Preliminary report on the paleomagnetism of 1.8 Ga dykes from the Bastar and Dharwar cratons, Peninsular India. *Gondwana Res.*, 2011, **20**, 335–343.
16. Pradhan, V. R., Meert, J. G., Pandit, M. K., Kamenov, G. and Mondal, M. E. A., Paleomagnetic and geochronological studies of the mafic dyke swarms of Bundelkhand craton, central India: implications for the tectonic evolution and paleogeographic reconstructions. *Precambrian Res.*, 2012, **198–199**, 51–76.
17. Radhakrishna, T., Ram Chandra, Srivastava, A. and Balasubramonian, G., Central Indian Bundelkhand and Bastar cratons in the Palaeoproterozoic supercontinental reconstructions: a palaeomagnetic perspective. *Precambrian Res.*, 2013, **226**, 91–104; doi.org/10.1016/j.precam res.2012.11.013
18. Radhakrishna, T., Krishnendu, N. R. and Balasubramonian, G., Palaeoproterozoic Indian shield in the global continental assembly: evidences from palaeomagnetism of mafic dykes. *Earth-Sci. Rev.*, 2013, **126**, 370–389.
19. Belica, M. E. *et al.*, Palaeoproterozoic mafic dyke swarms from the Dharwar craton; 3 paleomagnetic poles for India from 2.37–1.88 Ga and rethinking the Columbia 4 supercontinent. *Precambrian Res.*, 2014, **244**, 100–122.
20. Ratre, K., De Waele, B., Biswal, T. K. and Sinha, S., SHRIMP geochronology for the 1450 Ma Lakhna dyke swarm: its implication for the presence of Eoarchaean crust in the Bastar Craton and 1450–517 Ma depositional age for Purana basin (Khariar), Eastern Indian Peninsula. *J. Asian Earth Sci.*, 2010, **39**, 565–577.
21. Roy, A. and Prasad, M. H., Tectonothermal events in Central Indian Tectonic Zone (CITZ) and its implications in Rodinian crustal assembly. *J. Asian Earth Sci.*, 2003, **22**, 115–129.
22. Yedekar, D. B., Jain, S. C., Nair, K. K. K. and Dutta, K. K., *The Central Indian Collision Suture, Precambrian of Central India*, Geological Society India Special Publication, 1990, **57**, 9–25.
23. Roy, A., Kagami, H., Yoshida, M., Roy, A., Bandyopadhyay, B. K. and Chattopadhyay, A., Rb/Sr and Sm/Nd dating of different metamorphic events from the Sausar mobile belt, central India;

implications for Proterozoic crustal evolution. *J. Asian Earth Sci.*, 2006, **26**, 61–76.

24. Radhakrishna, T., Ram Chandra, Srivatava, A. K., Balasubramonian, G. and Balakrishna, S., Palaeoproterozoic mafic (dyke) activity in Bundelkhand craton, India and tectonic implications. In Proceedings of the Second Precambrian Crustal Growth and Tectonism, Bundelkhand University, Jhansi, absrt. LA4, 2009.
25. Naqvi, S. M., Enigma of Eo- and Palaeo-Archaean crustal evolution; constraints from Mesoarchaean cratonic parts of India: a global review. *Geol. Soc. India Mem.*, 2008, **74**, 1–31.
26. Ramakrishnan, M. and Vaidyanadhan, *Geology of India (vol. 1)*, Geological Society of India, Bangalore, 2008, p. 556.
27. Ramakrishnan, M., Nanda, J. K. and Augustine, P. F., *Geological Evolution of the Proterozoic Eastern Ghats Mobile Belt*, Geological Survey of India Special Publication, 1998, No. 44, pp. 1–21.
28. Vijaya Kumar, K. and Leelanandam, C., Evolution of the Eastern Ghats Belt, India: a plate tectonic perspective. *J. Geol. Soc. India*, 2008, **72**, 720–749.
29. Radhakrishna, B. P., Purana Basins of India. *Geol. Soc. India, Mem.*, 1987, 6.
30. French, J. E., Heaman, L. M., Chacko, T. and Srivastava, R. K., 1891–1883 Ma Southern Bastar-Cuddapah mafic igneous events, India: a newly recognised large igneous province. *Precambrian Res.*, 2008, **160**, 308–322.
31. Nanda, J. K., Rath, S. C. and Behera, S. N., Alkaline and Ultramafic magmatism in the Contact Zone between High and Low Grade Terrains: Example from NW Orissa, India: Precambrian Crust in Eastern and Central India. Geological Survey of India, Bhubaneswar, 1998, pp. 122–130.
32. Radhakrishna, T., Pearson, D. G. and Mathai, J., Evolution of Archaean southern Indian lithospheric mantle: a geochemical study of Proterozoic Agali – Coimbatore dykes. *Contrib. Mineral. Petrol.*, 1995, **121**, 351–363; doi:10.1007/s004100050101.
33. Radhakrishna, T., Balasubramonian, G., Joseph, M. and Krishnendu, N. R., Mantle processes and geodynamics: inferences from mafic dykes of South India. In *Earth System Science and Natural Resource Management*, Centre for Earth Science Studies, Trivandrum, 2004, pp. 3–25.
34. Radhakrishna, T. and Joseph, M., Geochemistry and petrogenesis of the Proterozoic dykes in Tamil Nadu, South India: implications for the continental lithosphere *Geol. Rundsch*., 1998, **87**, 268–282.
35. Radhakrishna, T., Precambrian mafic magmatism in South Indian Granulite Terrain. *J. Geol. Soc. India*, 2009, **73**, 131–142; doi:10.1007/s12594-009-0008-x
36. Srivastava, R. K., Hall, R. P., Verma, R. and Singh, R. K., Contrasting mafic dykes of the Bastar craton, central India: petrological and geochemical characteristics. *J. Geol. Soc. India*, 1996, **48**, 537–546.
37. Srivastava, R. K. and Gautam, G. C., Precambrian mafic magmatism in the Bastar Craton, Central India. *J. Geol. Soc. India*, 2009, **73**, 52–72.
38. Mondal, M. E. A. and Talat, A., Bundekhand mafic dykes, Central Indian shield: implication for the role of sediments subduction in Proterozoic crustal evolution. *Island Arc*, 2001, **10**, 51–67.
39. McFadden, P. L. and McElhinny, M. W., Classification of the reversal test in paleomagnetism. *Geophys. J. Int.*, 1990, **103**, 725–729.
40. Klootwijk, C. T., A review of palaeomagnetic data from the Indo-Pakistani fragment of Gondwanaland. In *Geodynamics of Pakistan* (Fara, A. and Dejong, K. A.), Geological Survey of Pakistan, Quetta, 1979, pp. 41–80.
41. Radhakrishna, T., Joseph, M., Krishnendu, N. R. and Balasubramonian, G., Palaeomagnetism of mafic dykes in the Karnataka Craton: possible geodynamic implications. *Geol. Soc. India Mem.*, 2003, **50**, 93–224.
42. Buchan, K. L., Pole, key paleomagmetic. In *Encyclopaedias of Geomagnetism and Paleomagnetism* (eds Gibbins, D. and Herrero-Bervera, E.), Springer, Dordrecht, The Netherlands, 2007, pp. 839–840.
43. Evans, D. A. D. and Pisarevsky, S. A., Plate tectonics on the early Earth?-weighing the paleomagnetic evidence. In *When Did Plate Tectonics Begin: Geological Society of America Special Paper*, (eds Condie, K. and Pease, V.), 2008, vol. 440, pp. 249–263.
44. Dash, J. K., Pradhan, S. K., Bhutani, R., Balakrishnan, S., Chandrasekaran, G. and Basavaiah, N., Palaeomagnetism of ca. 2.3 Ga mafic dyke swarms in the northeastern Southern Granulite Terrain, India: Constraints on the position and extent of Dharwar craton in the Palaeoproterozoic. *Precambrian Res.*, 2013; doi:10.1016/j.precamres.2013.01.004.
45. Stein, H. J., Hannah, J. L., Zimmerman, A., Markey, R. J., Sarkar, S. C. and Pal, A. B., A 2.5 Ga porphyry Cu–Mo–Au deposit at Malanjhkhand, central India: implications for late Archean continental assembly. *Precambrian Res.*, 2004, **134**, 189–226.
46. Pandey, U. K., Sastry, D. V. L. N., Pandey, B. K., Maduparna Roy, Rawat, T. P. S., Ranjan, R. and Shrivastava, V. K., Geochronological (Rb–Sr and Sm–Nd) studies on intrusive gabbros and dolerite dykes from parts of northern and central Indian cratons: implications for the age of onset of sedimentation in Bijawar and Chattisgarh basins and uranium mineralization. *J. Geol. Soc. India*, 2012, **79**, 30–40.
47. Rao, J. M., Rao, G. V. S. P., Widdowson, M. and Kelley, S. P., Evolution of Proterozoic mafic dyke swarms of the Bundelkhand Granite Massif, Central India. *Curr. Sci*., 2005, **88**, 502–506.
48. Sarkar, A. and Mallik, A. K., Geochronology and geochemistry of Precambrian mafic dykes from Kolar gold field, Karnataka. *Mem. Geol. Soc. India*, 1995 **25**, 111–132.
49. Radhakrishna, T., Maluski, H., Mitchell, J. G. and Joseph, M., K–Ar and $^{40}Ar/^{39}Ar$ isotope geochronology of the dykes from the south Indian granulite terrain. *Tectonophysics*, 1999, **304**, 109–129.
50. Hoffman, P. F., United plates of America, the birth of a craton. *Ann. Rev. Earth Planet. Sci*., 1988, **16**, 543–603.
51. Gower, C. F., Schärer, U. and Heaman, L. M., The Labradorian Orogeny in the Grenville Province, eastern Labrador. *Can. J. Earth Sci.*, 1992, **29**, 1944–1957.
52. Krapez, B., Stratigraphic record of an Atlantic-type global tectonic cycle in the Palaeoproterozoic Ashburton Province of Western Australia. *Aust. J. Earth Sci.*, 1999, **46**, 71–87.
53. Rogers, J. J. W., A history of the continents in the past three billion years. *J. Geol.*, 1996, **104**, 91–107.
54. Condie, K. C., Breakup of a Palaeoproterozoic supercontinent. *Gondwana Res.*, 2002, **5**, 41–43.
55. Hou, G., Santosh, M., Qian, X., Lister, G. S. and Li, J., Configuration of the Late Paleoproterozoic supercontinent Columbia: insights from radiating mafic dyke swarms. *Gondwana Res*., 2008, **14**, 395–409.
56. Zhao, G. C., Sun, M. and Wilde, S. A., Correlations between the Eastern Block of the North China Craton and the South Indian Block of the Indian Shield: an Archean to Paleoproterozoic link. *Precambrian Res.*, 2003, **122**, 201–233.
57. Piper, J. D. A., Zhang, J., Baochung, H. and Roberts, A. P., Palaeomagnetism of Precambrian dyke swarms in the North China shield: the 1.8 Ga LIP event and crustal consolidation in late Palaeoproterozoic times. *J. Asian Earth Sci.*, 2011, **41**, 504–524.
58. Zhang, S., Li, Z.-X., Evans, D. A. D., Wu, H., Li, H. and Dong, J., Pre-Rodinia supercontinent Nuna shaping up: a global synthesis with new palaeomagnetic results from North China. *Earth Planet. Sci. Lett.*, 2012, **353–354**, 145–155.
59. Lambecka, A., Barovichb, K., Gibsona, G., Hustona, D. and Pisarevsky, S., An abrupt change in Nd isotopic composition in Australian basins at 1655 Ma: implications for the tectonic evolution of Australia and its place in NUNA. *Precambrian Res*., 2012, **208–211**, 213–221.
60. Rasmussen, B., Bose, P. K., Sarkar, S., Banerjee, S., Fletcher, I. R. and Mcnaughton, N. J., 1.6 Ga U–Pb zircon age for the Chorhat

Sandstone, lower Vindhyan, India: possible implications for early evolution of animals. *Geology*, 2002, **30**, 103–106.
61. Ray, J. S., Martin, M. W., Veizer, J. and Bowring, S. A., U–Pb zircon dating and Sr isotope systematics of the Vindhyan Supergroup, India. *Geology*, 2002, **30**, 131–134.
62. Brewer, T. S., Daly, J. S. and Åhäll, K., Contrasting magmatic arcs in the Palaeoproterozoic of the south-western Baltic Shield. *Precambrian Res*., 1998, **92**, 297–315.
63. Åhäll, K.-I. and Connelly, J. N., Long-term convergence along SW Fennoscandia: 330 m.y. of Proterozoic crustal growth. *Precambrian Res.*, 2008, **163**, 402–421.
64. Sun, S. S. and McDonough, W. F., Chemical and isotope systematics of oceanic basalts: implication for mantle composition and processes. *Geol. Soc. Am. Spec. Publ*., 1989, **42**, 313–345.
65. Radhakrishna, T. and Joseph, M. Proterozoic palaeomagnetism of the mafic dyke swarms in the high-grade region of south India. *Precambrian Res*., 1996, **76**, 31–46.
66. Radhakrishna, T., Rao, G. V. S. P., Mitchell, J. G. and Venkatesh, A. S., Proterozoic basic dyke activity in Kerala along the western continental margin of India. *J. Geol. Soc. India*, 1986, **27**, 245–253.
67. Hargraves, R. B. and Bhalla, M. S., Precambrian palaeomagnetism in India through 1982: a review. *Geol. Soc. India Mem*., 1983, **4**, 491–524.
68. Halls, H. C., Li, J., Davis, D., Hou, G., Zhang, B. and Qian, X., A precisely dated Proterozoic palaeomagnetic pole from the North China craton, and its relevance to palaeocontinental reconstruction. *Geophys. J. Int*., 2000, **143**, 185–203.
69. Wu, H., Zhang, S., Li, Z. X., Li, H. and Dong, J., New paleomagnetic results from the Yangzhuang Formation of the Jixian System, North China, and tectonic implications. *Chin. Sci. Bull*., 2005, **50**, 1483–1489.
70. Zhang, H. M. and Zhang, W. Z., Paleomagnetic data, late Precambrian magnetostratigraphy and tectonic evolution of eastern China. *Precambrian Res*., 1985, **29**, 65–75.
71. Wu, H., New paleomagnetic results from Mesoproterozoic successions in Jixian Area, North China Block, and their implications for paleocontinental reconstructions. China University of Geosciences, Beijing, 2005, p. 133.
72. Halls, H. C. and Heaman, L. M., The paleomagnetic significance of new U–Pb age data from the Molson dyke swarm, Cauchon Lake area, Manitoba. *Can. J. Earth Sci*., 2000, **37**, 957–966.
73. Park, J. K., Irving, E. and Donaldson, J. A., Paleomagnetism of the Dubawnt Group. *Geol. Soc. Am. Bull*., 1973, **84**, 859–870.
74. Irving, E., Baker, J., Hamilton, M. and Wynne, P. J., Early Proterozoic geomagnetic field in western Laurentia: implications for paleolatitudes, local rotations and stratigraphy. *Precambrian Res*., 2004, **129**, 251–270.
75. McGlynn, J. C., Hanson, G. N., Irving, E. and Park, J. K., Paleomagnetism and age of Nonacho Group sandstones and associated Sparrow dikes, District of Mackenzie. *Can. J. Earth Sci.*, 1974, **11**, 30–42.
76. Larson, E. E., Reynolds, R. and Hoblitt, R., New virtual and paleomagnetic pole positions from isotopically dated Precambrian rocks in Wyoming, Montana and Arizona: their significance in establishing a North American apparent polar wandering path. *Geol. Soc. Am. Bull.*, 1973, **84**, 3231–3248.
77. Emslie, R. F., Irving, E. and Park, J. K., Further paleomagnetic results from the Michikamau intrusion, Labrador. *Can. J. Earth Sci*., 1976, **13**, 1052–1057.
78. Meert, J. G. and Stuckey, W., Revisiting the paleomagnetism of the 1.476 Ga St. Francois Mountains igneous province, Missouri. *Tectonics*, 2002, **21**, 1007.
79. Buchan, K. L., Ernst, R. E., Hamilton, M. A., Mertanen, S., Pesonen, L. J. and Elming, S.-A., Rodinia: the evidence from integrated palaeomagnetism and U–Pb geochronology. *Precambrian Res*., 2001, **110**, 9–32.
80. Elston, D. P., Enkin, R. J., Baker, J. and Kisilevsky, D. K., Tightening the belt: paleomagnetic–stratigraphic constraints on deposition, correlation, and deformation of the Middle Proterozoic (*ca.* 1.4 Ga) Belt–Purcell Supergroup, United States and Canada. *Geol. Soc. Am. Bull*. 2002, **114**, 619–638.
81. Buchan, K. L., Mertanen, S., Park, R. G., Pesonen, L. J., Elming, S.-A., Abrahamsen, N. and Bylund, G., Comparing the drift of Laurentia and Baltica in the Proterozoic: the importance of key palaeomagnetic poles. *Tectonophysics*, 2000, **319**, 167–198.
82. Evans, D. A. D. and Mitchell, R. N., Assembly and breakup of the core of Paleoproterozoic–Mesoproterozoic supercontinent Nuna. *Geology*, 2011, **39**, 443–446.
83. Idnurm, M., Precambrian palaeolatitudes for Australia – an update. Report prepared for Geoscience Australia, Canberra, 2004, p. 20.
84. Williams, G. E., Schmidt, P. W. and Clark, D. A., Palaeomagnetism of iron-formation from the late Palaeoproterozoic Frere Formation, Earaheedy Basin, Western Australia: palaeogeographic and tectonic implications. *Precambrian Res.*, 2004, **128**, 367–383.
85. Li, Z. X., Guo, W. and Powell, C. M., Timing and genesis of Hamersley BIF-hosted iron deposits: a new palaeomagnetic interpretation. MERIWA Project M242, Minerals and Energy Research Institute of Western Australia Report No. 199, 2000, p. 216.
86. McElhinny, M. W. and Evans, M. E., Palaeomagnetic results from the Hart dolerite of the Kimberley Block, Australia. *Precambrian Res.*, 1996, **3**, 231–241.
87. Li, Z. X., Palaeomagnetic evidence for unification of the north and west Australian cratons by *ca.* 1.7 Ga. New results from the Kimberley basin of northwestern Australia. *Geophys. J. Int*., 2000, **142**, 173–180.
88. Idnurm, M., Towards a high resolution Late Palaeoproterozoic–earliest Mesoproterozoic apparent polar wander path for northern Australia. *Aust. J. Earth Sci*., 2000, **47**, 405–429.
89. Idnurm, M., Giddings, J. W. and Plumb, K. A., Apparent polar wander and reversal stratigraphy of the Palaeo–Mesoproterozoic southeastern McArthur Basin, Australia. *Precambrian Res*., 1995, **72**, 1–41.
90. Pisarevsky, S. A., Wingate, M. T. D., Powell, C. M., Johnson, S. and Evans, D. A. D., Models of Rodinia assembly and fragmentation. *Geol. Soc. Spec. Publ., London*, 2003, **206**, 35–55.
91. Lubnina, N. V., Mertanen, S., Soderlund, U., Bogdanova, S. V., Vasilieva, T. I. and Frank-Kamenetsky, D., A new key pole for the East European Craton at 1452 Ma: palaeomagnetic and geochronological constraints from mafic rocks in the Lake Ladoga region. *Precambrian Res.*, 2010, **183**, 442–462.
92. Didenko, A. N. *et al*., Palaeomagnetism and U–Pb dates of the Palaeoproterozoic Akitkan Group (South Siberia) and implications for pre-Neoproterozoic tectonics. *Geol. Soc. Spec. Publ., London*, 2009, 145–163.

ACKNOWLEDGEMENTS. This paper is an outcome of the Department of Science and Technology, Government of India funded projects (DST sanction no: ESS-16-196-2003; ESS/16/090/97) and joint collaborative project between the National Centre for Earth Science Studies (NCESS), Thiruvananthapuram and Centre of Excellence (CoE) in Geology, Institute of Earth Science, Bundelkhand University (BU), Jhansi. We are thank NCESS and CoE, BU for permission to carry out this research work. We also thank Dr M. Ramakrishnan (former Deputy Director General, Geological Survey of India) for his suggestions to improve the manuscript, and Dr J.D.A. Piper (Liverpool University, UK) for his comments/corrections on the earlier version of this manuscript.

Received 5 January 2016; accepted 24 August 2016

doi: 10.18520/cs/v112/i04/811-822